Research Article Vol. 8, No. 4 / April 2021 / Optica 563

optica

Emulating exceptional-point encirclements using imperfect (leaky) photonic components: asymmetric mode-switching and omni-polarizer action

J. B. Khurgin,[1] Y. Sebbag,[2] E. Edrei,[2] R. Zektzer,[2] K. Shastri,[3] U. Levy,[2] and F. Monticone[3,*]

[1]Department of Electrical and Computer Engineering, Johns Hopkins University, Baltimore, Maryland 21218, USA
[2]Department of Applied Physics, The Center for Nanoscience and Nanotechnology, The Hebrew University of Jerusalem, Jerusalem 91904, Israel
[3]School of Electrical and Computer Engineering, Cornell University, Ithaca, New York 14853, USA
*Corresponding author: francesco.monticone@cornell.edu

Received 22 October 2020; revised 25 February 2021; accepted 15 March 2021 (Doc. ID 412981); published 16 April 2021

Non-Hermitian systems have recently attracted significant attention in photonics. One of the hallmarks of these systems is the possibility of realizing asymmetric mode-switching and omni-polarizer action through the dynamic encirclement of exceptional points (EPs). Here, we offer a new perspective on the operating principle of these devices, and we theoretically and experimentally show that linear asymmetric mode-switching and omni-polarizer action can be easily realized—with the same performance and limitations—using simple configurations that emulate the physics involved in encircling EPs without the complexity of actual encirclement schemes. The proposed concept of "encirclement emulators" and our theoretical and experimental results may allow better assessment of the limitations, practical potential, and applications of EP encirclements in non-Hermitian photonics.

https://doi.org/10.1364/OPTICA.412981

1. INTRODUCTION

Over the past two decades, the concept of parity–time (PT) symmetry has been at the center of attention in different areas of science and engineering, motivated by the realization that a system described by a non-Hermitian Hamiltonian can have real eigenvalues, as long as it commutes with the PT operator [1]. An entirely new discipline of non-Hermitian quantum mechanics has since been developed [2,3], with a particular focus on so-called exceptional points (EPs) [4], i.e., degeneracy points where two or more eigenvalues and eigenfunctions of the Hamiltonian coalesce. In this context, efforts on extending quantum mechanics to the complex domain have been hampered by the lack of experimental observation of PT-symmetric properties in the evolution of physical systems (to be more precise, while open quantum systems can be described by an effective non-Hermitian Hamiltonian [5], no physical system has been observed to evolve according to the CPT-inner product of PT-symmetric quantum theory [2]). Interestingly, however, PT symmetry turned out to be relatively easy to "synthesize" in classical wave-physics systems, especially in photonics, where non-Hermiticity arises from the presence of optical gain and/or loss, corresponding to the imaginary part of the dielectric constant (or radiation loss, parametric gain, etc.). Following the first pioneering theoretical works in this field [6–9], experimental observations of PT-symmetric phenomena in photonics, including EPs, were soon reported [10,11]. Since then, PT symmetry has been demonstrated in a large variety of photonic structures, including coupled waveguides, coupled resonators, lasers [12], Bragg gratings [13], etc. (more information can be found in extensive reviews [14–16]). In particular, the peculiar behavior of a system near EPs [17] has been observed and discussed in several papers. Notably, it has been shown that in the vicinity of an EP, the sensitivity of various sensors [18–20] can be enhanced due to the square-root branch-point nature of these degeneracies, suggesting that PT symmetry and EPs are more than just a fundamental physical concept, but may potentially be useful for relevant applications.

One of the most fascinating properties of PT-symmetric systems is the behavior of the eigenstates upon the encirclement of an EP through a variation of the system's parameters in space or time. Adiabatic encirclement of EPs was first studied in [21,22], and it was predicted that each time an adiabatic encirclement takes place, it will cause a flip of the eigenstates. This state-flipping behavior has been confirmed in a number of "quasi-static" experiments where the eigenstates were monitored under stationary conditions while discretely changing the parameters of the system [23–25]. However, more recently, it was shown theoretically that when the encirclement occurs dynamically, the fact that the Hamiltonian of the system is non-Hermitian (i.e., in optics, it involves loss and/or gain) prevents one from applying the adiabatic theorem, and the encirclement of the EP results in a final state that depends only on the direction (helicity) of the encirclement and not on

the initial state [26–29]. This behavior suggests intriguing implications for multi-port or multi-mode devices whose output is independent of the input state. The dynamic encirclement was first experimentally demonstrated in 2016 in non-Hermitian (lossy) microwave waveguides with coupled modes, resulting in asymmetric mode switching [30]. Very recently, this concept of dynamic EP encirclement was also proposed to realize a linear asymmetric omni-polarizer, in which arbitrarily polarized input light always exits the system in a certain fixed polarization state going in one direction and in the orthogonal state going in the opposite direction. This idea was originally proposed in [29] and experimentally demonstrated in [31]. While omni-polarizers have already been designed and demonstrated based on *nonlinear* effects, for example, using optical fiber nonlinearities in [32], the recent works in [29,31] focused, instead, on the possibility of realizing *linear* asymmetric omni-polarizers using EP encirclements. These first results on asymmetric mode-switching and omni-polarizer action have understandably generated a certain amount of excitement for the development of robust linear photonic devices based on dynamic EP encirclement. We believe it is therefore important to assess the practicality of these devices as well as their uniqueness, i.e., to answer the question about whether the desired functionality can be achieved only by dynamic EP encirclement, and not with simpler photonic schemes. In this paper, we answer these relevant questions based on general theoretical considerations and proof-of-concept experiments. We show that linear dynamic-encirclement devices suffer from a major inherent drawback: while their output state is indeed mostly independent of their input state, their transmission amplitude necessarily exhibits a very strong dependence on the input state. Furthermore, we demonstrate experimentally that asymmetric mode-switching performance virtually identical to dynamic encirclement schemes can be achieved in far simpler optical systems using a few standard linear components such as couplers, beam splitters, and waveplates, and whose operational principle can be understood without involving EPs. Incidentally, we note that analogous approaches, using standard beam splitters, phase shifters, mode-selective loss/gain, etc., have been used in the past to emulate PT-symmetric quantum dynamics and other effects in non-Hermitian wave physics [33–35]; however, to the best of our knowledge, the present work is the first to demonstrate the emulation of EP encirclements for asymmetric mode-switching and omni-polarizer action.

2. RECIPROCITY AND TRANSMISSION-MATRIX ASYMMETRY

The recently proposed and experimentally demonstrated asymmetric mode switches [30] and omni-polarizers [29,31] are linear reciprocal devices that produce a certain output state (A) in the forward direction, regardless of the input state (A or B), whereas they produce the opposite output state (B) in the backward direction, again independent of the input state. State (A) or (B) can be a certain waveguide mode, polarization state, or any other state belonging to a set of orthogonal channels, e.g., a state of angular momentum.

The transmission properties of an asymmetric two-port linear device, as in Fig. 1(a), can be described by a 2×2 transmission matrix (composed of the transmission elements of the scattering matrix; not to be confused with the transfer matrix or characteristic matrix):

$$T^{\rightarrow} = \begin{pmatrix} T_{AA}^{\rightarrow} & T_{BA}^{\rightarrow} \\ T_{AB}^{\rightarrow} & T_{BB}^{\rightarrow} \end{pmatrix}. \tag{1}$$

The device may contain gain and/or loss; hence, there is no passivity constraints on the magnitudes of the transmission coefficients, i.e., the scattering matrix is not unitary. The device, however, is assumed to be reciprocal; hence, the transmission matrix in the backward direction is

$$T^{\leftarrow} = \begin{pmatrix} T_{AA}^{\leftarrow} & T_{BA}^{\leftarrow} \\ T_{AB}^{\leftarrow} & T_{BB}^{\leftarrow} \end{pmatrix} = \begin{pmatrix} T_{AA}^{\rightarrow} & T_{AB}^{\rightarrow} \\ T_{BA}^{\rightarrow} & T_{BB}^{\rightarrow} \end{pmatrix}. \tag{2}$$

Consider a device designed to produce output A when excited from the left and output B when excited from the right. Reciprocity (symmetry of the scattering matrix) imposes severe constraints on the operation of such a device. In particular, an ideal asymmetric mode switch, with transmission amplitude in a

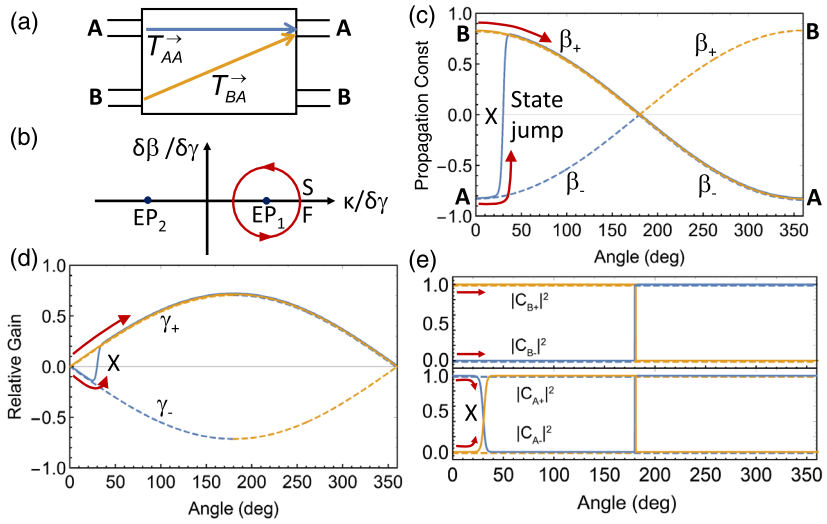

Fig. 1. (a) Two-port linear system under study: ports A and B may correspond to different guided modes or polarization states. (b) EPs and encirclement trajectory. Evolution during encirclement of (c) relative propagation constants, (d) relative gain (dashed curves: eigensolutions; solid curves: eigensolutions weighted by the respective population coefficient), and (e) population coefficients for the system initially prepared in mode B (top) and mode A (bottom). Red arrows indicate the direction of encirclement.

certain output state *equal* for both input states, for both excitation directions, must be nonreciprocal. To understand this better, let us assume a unity transmission coefficient from port B on the left to port A on the right, i.e., $T_{BA}^{\rightarrow}=1$; then, it is necessary that $T_{AA}^{\rightarrow}=\alpha$, with $\alpha \ll 1$ if the device is to produce (mostly) output B in the opposite direction. Indeed, because of reciprocity, $T_{AB}^{\leftarrow}=T_{BA}^{\rightarrow}=1$ and $T_{AA}^{\leftarrow}=T_{AA}^{\rightarrow}=\alpha$. Therefore, if $\alpha=1$, the device can operate as an ideal mode switch or omni-polarizer in the forward direction, with identical transmission amplitude for both input states (A or B), but it would then act as a signal splitter in the backward direction. In even simpler terms, an ideal mode switch or omni-polarizer must be described by a forward transmission matrix:

$$T^{\rightarrow}=\begin{pmatrix}1 & 1\\ 0 & 0\end{pmatrix}, \tag{3}$$

which, however, would imply that, since the device is reciprocal, the backward transmission matrix would be

$$T^{\leftarrow}=\begin{pmatrix}1 & 0\\ 1 & 0\end{pmatrix}, \tag{4}$$

which is not an omni-polarizer or mode switch, but a mode filter (suppressing input B) followed by a 3 dB mode splitter, i.e., something of dubious utility. Consistent with this discussion, experimental results for the asymmetric mode switch in [30] indeed show strongly input-dependent transmission with $T_{BA}^{\rightarrow}/T_{AA}^{\rightarrow}=1/\alpha=28$ dB and $T_{AB}^{\rightarrow}/T_{BB}^{\rightarrow}=14$ dB. Assuming that one can bring $T_{BA}^{\rightarrow}$ to unity using optical amplifiers, the fact that insertion loss for one of the input states is as high as nearly 30 dB puts practicality of such a device in doubt.

Thus, any linear reciprocal device designed to operate as an *asymmetric* mode switch or *asymmetric* omni-polarizer must have transmission amplitude that is strongly dependent on the input state. This is true regardless of the device implementation, and it follows directly from reciprocity. In light of these considerations, we argue that if only reciprocal linear components are used, there are much simpler ways to obtain the same asymmetric mode-switching action than dynamic encirclement of EP's.

3. EXCEPTIONAL-POINT ENCIRCLEMENTS AND THEIR EMULATION

Let us now try to understand the basic physical principle that causes asymmetric mode switching during an EP encirclement, and whether this process can be emulated. For two coupled modes $E_{1,2}$ with complex propagation constants $\beta_{1,2}+i\gamma_{1,2}$, the basic, yet rather prolific, characteristic matrix (Hamiltonian) that is essentially at the basis of the entire PT-symmetry field is

$$H=\bar{H}+H_{\text{int}}=\begin{pmatrix}\bar{\beta}+i\bar{\gamma} & 0\\ 0 & \bar{\beta}+i\bar{\gamma}\end{pmatrix}+\begin{pmatrix}\delta\beta+i\delta\gamma & \kappa\\ \kappa & -\delta\beta-i\delta\gamma\end{pmatrix}, \tag{5}$$

where κ is the coupling coefficient, $\bar{\beta}=(\beta_1+\beta_2)/2$, $\bar{\gamma}=(\gamma_1+\gamma_2)/2$, $\delta\beta=(\beta_1-\beta_2)/2$, and $\delta\gamma=(\gamma_1-\gamma_2)/2$. The two complex eigensolutions, $\tilde{\beta}_{\pm}=\bar{\beta}+i\bar{\gamma}\pm\sqrt{(\delta\beta+i\delta\gamma)^2+\kappa^2}$, reveal two EP's [shown in Fig. 1(b)] for $\delta\beta=0$ and $\kappa=\pm\delta\gamma$, at which two solutions have identical eigenvalues and eigenvectors.

Let us then consider what happens when we encircle one of the EPs, counterclockwise from a starting point S to a final point $F=S$. The results are shown in Figs. 1(c)–1(e) for an encirclement along the contour with radius $0.3\delta\gamma$. In Figs. 1(c) and 1(d), one can see the evolution of the relative propagation constant, $\beta_{\pm}=\text{Re}(\tilde{\beta}_{\pm})-\bar{\beta}$, and the relative gain, $\gamma_{\pm}=\text{Im}(\tilde{\beta}_{\pm})-\bar{\gamma}$, while Fig. 1(e) shows the evolution of the population coefficients $|C_{A,B\pm}|^2$, i.e., the projection of the instantaneous state vector along the instantaneous eigenvectors $E_{\pm}(\theta)$. If we initially prepare the system in one of the eigenstates, $E_{-}(0)$(or $E_{+}(0)$), associated with mode $A(B)$, and assuming full adiabaticity, the mode should be converted into mode $B(A)$ as a result of a full parametric encirclement. However, as the two instantaneous eigenstates evolve, they experience very different relative gain/loss; in addition, due to the non-Hermitian nature of the problem, the eigenstates are not strictly orthogonal, and a portion of energy may leak from one state to the other. In particular, a leakage from the lossy state (originating from A; see Fig. 1) to the amplifying state cannot be ignored, as this fraction of energy will then experience a relative gain, while the remaining fraction in the lossy state will suffer extinction. This induces a state jump around point X in Fig. 1, consistent with [29,30] (the location of point X depends on the degree of non-adiabaticity, i.e., the speed of dynamic encirclement). As a result, toward the end of a full dynamic encirclement, the optical signal originating from A will be much stronger in mode A than in mode B. Conversely, the light that leaked from the amplifying state, originating from B, into the lossy state would suffer extinction and can be neglected (no state jump occurs in this case). Hence, no matter where the signal originates (i.e., its input state), it ends up mostly in mode A, as indicated by the solid curves in Figs. 1(c)–1(e). Following the same reasoning, it is also clear that reversing the direction of encirclement (or of propagation) will bring the signal mostly into mode B, regardless of the input state. This is the mechanism behind the asymmetric mode-switching effect in [30]. However, it is also important to recognize that when dynamic encirclement takes place along one trajectory (going from B to A), the entire signal propagates with relative gain, while along the other possible trajectory with the same output (going from A to A), at first the signal experiences a large loss (attenuation and leakage), and then it gets recovered by experiencing relative amplification. This combination of high loss followed by high gain may look benign to a theorist, yet it appears noxious in practice since the signal-to-noise ratio (SNR) is greatly deteriorated.

At this point, an astute reader may have noted that since all the "modal-switching" action takes place in the vicinity of point X, the relative gain/loss preceding and following it does not have to be distributed and can simply be formed by lumped optical amplifiers and attenuators. Theoretically speaking, in the absence of gain/loss, adiabaticity for slowly varying systems tends to get restored, but in any real system, ideal adiabaticity is never fully achieved. It is precisely this fact (leakage due to imperfect adiabaticity) that makes the remarkable properties of dynamic encirclement possible, while the specific evolution of the eigenmodes before/after point X is insignificant, as long as different trajectories have different gain and loss. Based on these considerations, it is clear that essentially the same behavior can be observed and emulated by using a leaky mode coupler preceded and followed by lumped gain/loss elements. As illustrated in Fig. 2(a), the coupler can simply be an imperfect directional coupler with coupling coefficient $|\kappa|<1$, preceded and followed by optical amplifiers and optical attenuators (using two different levels of loss would also work). The transmission matrices for the proposed "encirclement emulator" are

$$T^{\rightarrow} = \begin{pmatrix} 1-\kappa^2-\gamma_1+\gamma_4 & \kappa^2+\gamma_3+\gamma_4 \\ \kappa^2-\gamma_1-\gamma_2 & 1-\kappa^2-\gamma_2+\gamma_3 \end{pmatrix},$$

$$T^{\leftarrow} = \begin{pmatrix} 1-\kappa^2-\gamma_1+\gamma_4 & \kappa^2-\gamma_1-\gamma_2 \\ \kappa^2+\gamma_3+\gamma_4 & 1-\kappa^2-\gamma_2+\gamma_3 \end{pmatrix} \quad (6)$$

for forward and backward propagation, respectively. The configuration in Fig. 2(a) offers a wide range of flexibility for obtaining the desired coupling ratios. For our experimental demonstration of such an "encirclement emulator," we have chosen to use no amplifiers, i.e., $\gamma_3 = \gamma_4 = 0$, a 3 dB optical coupler, $\kappa^2 = 0.5$, and attenuators with $\gamma_1 = 25$ dB and $\gamma_2 = 15$ dB, as shown in the illustration of our experimental setup in Fig. 2(b). The transmission matrix of the system is therefore

$$T^{\rightarrow} = \begin{pmatrix} -28\ \text{dB} & -3\ \text{dB} \\ -43\ \text{dB} & -18\ \text{dB} \end{pmatrix}, \quad T^{\leftarrow} = \begin{pmatrix} -28\ \text{dB} & -43\ \text{dB} \\ -3\ \text{dB} & -18\ \text{dB} \end{pmatrix}, \quad (7)$$

which clearly indicates that for forward (backward) propagation, the output is mostly in mode $A(B)$. The experiment was performed using a standard 3 dB fiber coupler and two variable optical attenuators (VOAs) in ports A-left and B-right, but an integrated version of the device can be easily envisioned. As illustrated in Fig. 2(b), a tunable laser source (New-port, Velocity TLB-6700) was injected separately through each port, while the intensity was measured at the outputs using a standard silicon detector (Thorlabs, DET100A). As the dynamic range of the detector is limited, pre-calibrated external filters were introduced and accounted for during post-processing when needed. To eliminate laser intensity fluctuations, a reference arm was used to normalize each measurement.

The experimental results are reported in Fig. 2(c), where all data points are presented relative to perfect transmission, i.e., without attenuators or coupling loss. If one compares these measurements with the corresponding ones for the dynamic encirclement scheme reported in [30], and replicated in Fig. 2(c), the results are virtually identical (except for the fact that our common insertion loss is more than 20 dB smaller): almost all forward (backward) propagating light ends up in mode A (B). Notice that the transmission amplitude is highly asymmetric in both our scheme and in [30], with $T^{\rightarrow}_{AA}/T^{\rightarrow}_{BA} = \alpha \approx -25$ dB, and $T^{\leftarrow}_{BB}/T^{\leftarrow}_{AB} \approx -15$ dB. As discussed above, this asymmetry is *unavoidable* in any linear and reciprocal asymmetric mode switch. The asymmetry can be mitigated by using nonlinear saturable amplifiers in positions γ_3 and γ_4, which simply add a certain power to the signal no matter what the input is. Then, a more uniform transmission amplitude for different inputs can be attained; however, this strategy would not alleviate the main impediment to practical applications, namely, the fact that the signal following one of the pathways initially suffers significant attenuation that deteriorates the SNR.

4. ASYMMETRIC OMNI-POLARIZER

The approach described in the previous section to emulate the effects of an EP encirclement can be easily applied to other tasks, such as to realize the linear asymmetric omni-polarizers first explored in [29] and recently realized in [31]. A possible configuration is shown in the dashed box in Fig. 3(a), based on two polarization-dependent gain/loss sections on the two sides of an *imperfect* half-wave plate, which assures that, rather than a complete swap of polarization components, there is leakage. In other

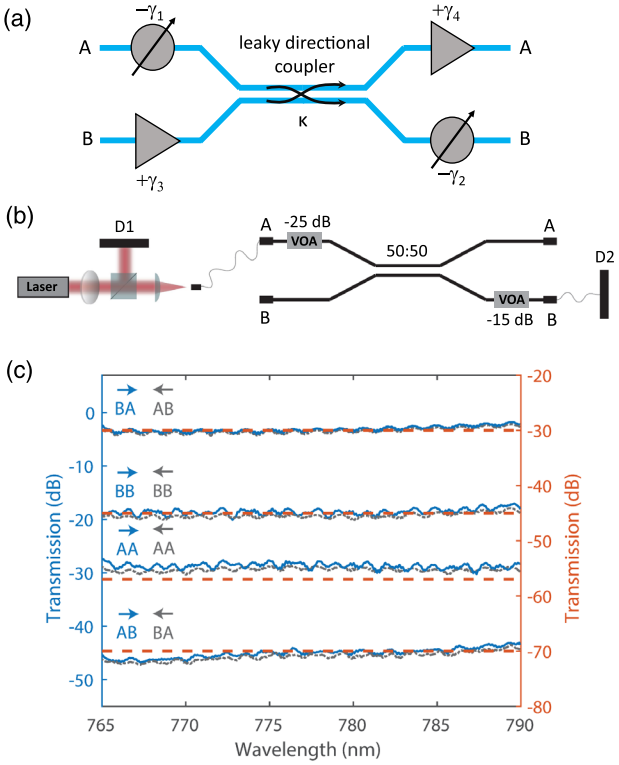

Fig. 2. (a) Proposed scheme realizing asymmetric mode switching, emulating a dynamic EP encirclement. (b) Experimental setup described in the main text. (c) Experimentally measured transmission amplitudes for a configuration as in (b) (solid blue and dotted gray lines correspond to the blue scale on the left axis), compared to the transmission amplitudes for the device in [30] (dashed orange lines correspond to the orange scale on the right axis; values taken at the central wavelength).

words, while a perfect half-wave plate, suitably oriented, would convert orthogonal polarization states into one another, an imperfect (leaky) half-wave plate is a device that performs this conversion only partially. Light is routed through this system using standard polarization beam splitters. For our experimental demonstration of this asymmetric omni-polarizer, we considered a more practical configuration, without amplifiers, i.e., $\gamma_3 = \gamma_4 = 0$, and we used optical attenuators with $\gamma_1 = \gamma_2 = 20$ dB, and a quarter-wave plate to simulate the effect of a leaky half-wave plate with a 50:50 ratio. These choices make our omni-polarizer design the direct equivalent of the asymmetric mode switch in Fig. 2(b), but operating on orthogonal polarization states instead of guided modes. As illustrated in Fig. 3(a), to select the desired input polarization state, the angle of the input linearly polarized light is controlled using a rotating non-leaky half-wave plate (or quarter-wave plate, as discussed in the following).

Figures 3(b) and 3(c) report the experimental measurements of the transmission amplitude in the two output polarization states for propagation from left to right and from right to left, respectively, as a function of the input linear-polarization state, namely, the angle of the rotating half-wave plate in Fig. 3(a). For the sake of clarity, we changed the notation of the channels from "A" and "B" (used for the asymmetric mode switch) to "V" and "H" denoting the vertical and horizontal linear polarization states. Considering Fig. 3(b) as an example, the top (bottom) solid curve is the measured transmission amplitude in the vertical (horizontal) linear-polarization channel, whereas the dashed lines are the

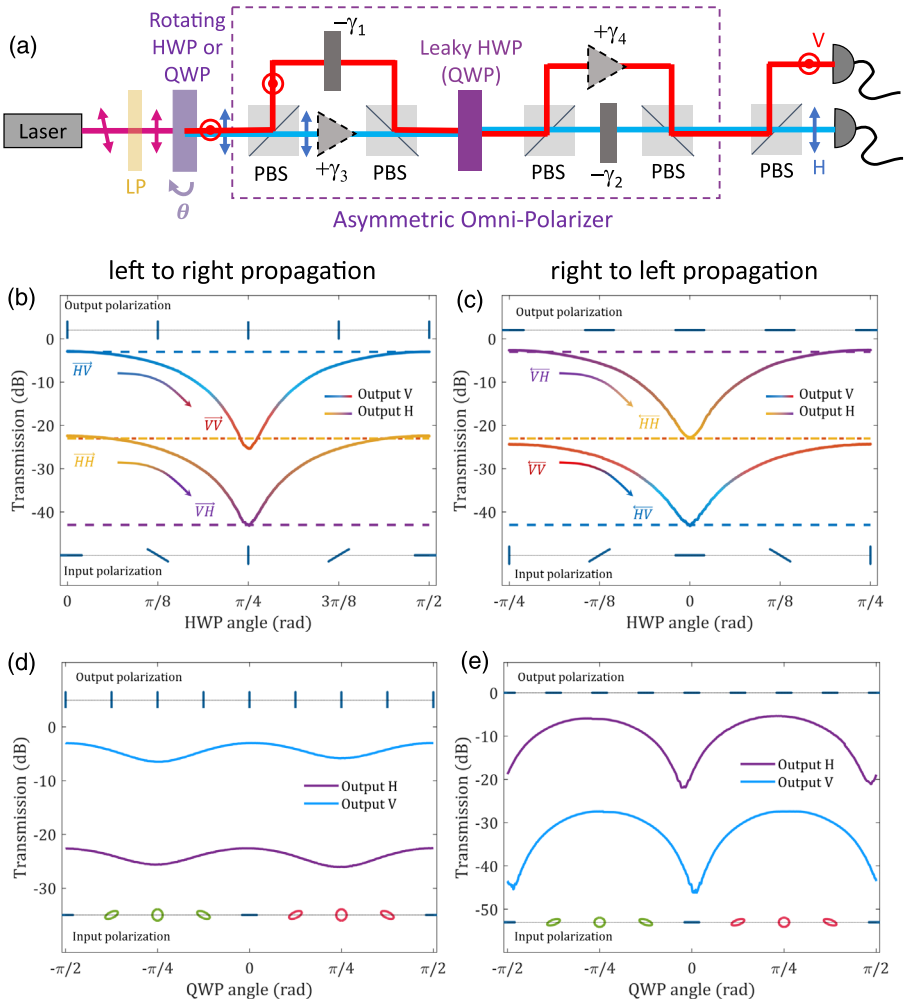

Fig. 3. (a) Proposed scheme to realize a linear asymmetric omni-polarizer, experimentally realized with off-the-shelf optical components. (b)–(e) Experimental results demonstrating the operation of the proposed device as an asymmetric omni-polarizer with large transmission asymmetry. Solid lines: experimentally measured transmission amplitude in the two output polarization states, i.e., horizontal (H) or vertical (V) linear polarization, for propagation from (b), (d) left to right and (c), (e) right to left as a function of the input linear-polarization state, namely, the angle of the (b), (c) rotating half-wave plate or (d), (e) quarter-wave plate in Fig. 3(a). Dashed lines in panels (b), (c): calculated elements of the transmission matrix for all possible input–output polarization "transformations": horizontal to vertical (blue), vertical to vertical (red), horizontal to horizontal (orange), and vertical to horizontal (purple). The color gradients in the solid curves in (b), (c) correspond to the colors of the dashed lines, indicating the change in polarization transformation, as described in the text. All panels also show the input and output polarization ellipses (normalized), obtained from experimental measurements.

calculated elements of the transmission matrix for all possible input–output polarization "transformations" (horizontal to vertical, vertical to vertical, horizontal to horizontal, and vertical to horizontal). The plots also show the input and output polarization ellipses. From the results in Figs. 3(b) and 3(c), it is clear that the output polarization state depends only on the propagation direction and not the input polarization: the transmission is much higher in the vertical polarization channel for propagation from left to right [Fig. 3(b)], whereas it is much higher in the horizontal polarization channel from right to left [Fig. 3(c)]. The same behavior is obtained if the input state is not linearly polarized, as we experimentally demonstrated by replacing the rotating half-wave plate in Fig. 3(a) with a rotating quarter-wave plate. The transmission measurements for this case are reported in Figs. 3(d) and 3(e), which further demonstrate that the output state is independent of the input state. All these experimental results show that the proposed device indeed operates as a linear asymmetric omni-polarizer. We also stress that this design is based on an operational mechanism far simpler than any schemes relying on EP encirclements, which require complex *ad hoc* structures and very long propagation lengths [29,31].

Most importantly, our experimental results in Figs. 3(b)–3(e) show that although this device operates as an omni-polarizer, the transmission amplitude is *strongly dependent* on the input state, which is perfectly in line with the performance of the asymmetric mode switch described in Section 3. Considering again Fig. 3(b) as an example, the top solid curve (vertical output) changes by more than 20 dB as the input polarization angle varies, while remaining approximately 20 dB higher than the other solid curve (horizontal output). The color of the top solid curve changes from blue to red to indicate that we go from a situation with horizontal-to-vertical polarization conversion (with high transmission) to a situation with vertical-to-vertical polarization conversion (with much lower transmission, but higher than the vertical-to-horizontal conversion). Thus, as expected, the asymmetric omni-polarizer inherits

the same limitations we discussed for the asymmetric mode switch in the previous section. We reiterate that such a large transmission asymmetry is inherent to any linear reciprocal device designed to act as an asymmetric mode switch or omni-polarizer, regardless of whether it is based on an actual EP encirclement or some other scheme, since these limitations originate directly from the reciprocity principle as discussed in Section 2.

5. CONCLUSION

In summary, based on theoretical considerations and experiments, we have shown that at least in optics, the effects of a dynamic EP encirclement on the system's transmission matrix are essentially indistinguishable from the effects of a signal leakage followed by large gain/loss asymmetry. Two sets of experiments, for an asymmetric mode switch and an asymmetric omni-polarizer, were performed using a small number of standard off-the-shelf optical components, demonstrating the same (or better) performance as actual encirclement schemes. The operation of these systems can be understood with straightforward theoretical considerations without involving the sophisticated theoretical concepts that are usually invoked when describing EP encirclements. Finally, we have shown that due to the inherent asymmetry of the transmission response, the SNR in all the "real" and "emulated" dynamic encirclement schemes is always expected to sharply deteriorate, for at least one of two input states, which, in our view, raises serious questions about the practical applicability of EP encirclement, but perhaps does not entirely preclude some niche applications depending on the specific requirements.

Funding. National Science Foundation (1741694); Air Force Office of Scientific Research (FA9550-19-1-0043); United States-Israel Binational Science Foundation (2016407).

Acknowledgment. J. B. K. would like to express deep gratitude to his colleagues Prof. P. Noir and Dr. S. Artois for unwavering support and stimulating discussions.

Disclosures. The authors declare no conflicts of interest.

Data Availability. Data underlying the results presented in this paper may be obtained from the authors upon reasonable request.

REFERENCES

1. C. M. Bender and S. Boettcher, "Real spectra in non-Hermitian Hamiltonians having PT symmetry," Phys. Rev. Lett. **80**, 5243–5246 (1998).
2. C. M. Bender, D. C. Brody, and H. F. Jones, "Complex extension of quantum mechanics," Phys. Rev. Lett. **89**, 270401 (2002).
3. N. Moiseyev, *Non-Hermitian Quantum Mechanics* (Cambridge University, 2011), p. xiii, 394 p.
4. W. D. Heiss, "Exceptional points of non-Hermitian operators," J. Phys. A **37**, 2455–2464 (2004).
5. M. Naghiloo, M. Abbasi, Y. N. Joglekar, and K. W. Murch, "Quantum state tomography across the exceptional point in a single dissipative qubit," Nat. Phys. **15**, 1232–1236 (2019).
6. A. Ruschhaupt, F. Delgado, and J. G. Muga, "Physical realization of -symmetric potential scattering in a planar slab waveguide," J. Phys. A **38**, L171–L176 (2005).
7. R. El-Ganainy, K. G. Makris, D. N. Christodoulides, and Z. H. Musslimani, "Theory of coupled optical PT-symmetric structures," Opt. Lett. **32**, 2632–2634 (2007).
8. Z. H. Musslimani, K. G. Makris, R. El-Ganainy, and D. N. Christodoulides, "Optical solitons in PT periodic potentials," Phys. Rev. Lett. **100**, 030402 (2008).
9. K. G. Makris, R. El-Ganainy, D. N. Christodoulides, and Z. H. Musslimani, "Beam dynamics in PT symmetric optical lattices," Phys. Rev. Lett. **100**, 103904 (2008).
10. A. Guo, G. J. Salamo, D. Duchesne, R. Morandotti, M. Volatier-Ravat, V. Aimez, G. A. Siviloglou, and D. N. Christodoulides, "Observation of PT-symmetry breaking in complex optical potentials," Phys. Rev. Lett. **103**, 093902 (2009).
11. C. E. Rüter, K. G. Makris, R. El-Ganainy, D. N. Christodoulides, M. Segev, and D. Kip, "Observation of parity–time symmetry in optics," Nat. Phys. **6**, 192–195 (2010).
12. H. Hodaei, M.-A. Miri, M. Heinrich, D. N. Christodoulides, and M. Khajavikhan, "Parity-time–symmetric microring lasers," Science **346**, 975–978 (2014).
13. L. Feng, M. Ayache, J. Huang, Y.-L. Xu, M.-H. Lu, Y.-F. Chen, Y. Fainman, and A. Scherer, "Nonreciprocal light propagation in a silicon photonic circuit," Science **333**, 729–733 (2011).
14. L. Feng, R. El-Ganainy, and L. Ge, "Non-Hermitian photonics based on parity–time symmetry," Nat. Photonics **11**, 752–762 (2017).
15. A. A. Zyablovsky, A. P. Vinogradov, A. A. Pukhov, A. V. Dorofeenko, and A. A. Lisyansky, "PT-symmetry in optics," Phys. Usp. **57**, 1063–1082 (2014).
16. J. Wen, X. Jiang, L. Jiang, and M. Xiao, "Parity-time symmetry in optical microcavity systems," J. Phys. B **51**, 222001 (2018).
17. S. Klaiman, U. Guenther, and N. Moiseyev, "Visualization of branch points in PT-symmetric waveguides," Phys. Rev. Lett. **101**, 080402 (2008).
18. W. Chen, Ş. Kaya Özdemir, G. Zhao, J. Wiersig, and L. Yang, "Exceptional points enhance sensing in an optical microcavity," Nature **548**, 192–196 (2017).
19. J. Wiersig, "Enhancing the sensitivity of frequency and energy splitting detection by using exceptional points: application to microcavity sensors for single-particle detection," Phys. Rev. Lett. **112**, 203901 (2014).
20. M. P. Hokmabadi, A. Schumer, D. N. Christodoulides, and M. Khajavikhan, "Non-Hermitian ring laser gyroscopes with enhanced Sagnac sensitivity," Nature **576**, 70–74 (2019).
21. O. Latinne, N. J. Kylstra, M. Dorr, J. Purvis, M. Teraodunseath, C. J. Joachain, P. G. Burke, and C. J. Noble, "Laser-induced degeneracies involving autoionizing states in complex atoms," Phys. Rev. Lett. **74**, 46–49 (1995).
22. A. A. Mailybaev, O. N. Kirillov, and A. P. Seyranian, "Geometric phase around exceptional points," Phys. Rev. A **72**, 014104 (2005).
23. C. Dembowski, H. D. Graf, H. L. Harney, A. Heine, W. D. Heiss, H. Rehfeld, and A. Richter, "Experimental observation of the topological structure of exceptional points," Phys. Rev. Lett. **86**, 787–790 (2001).
24. S. B. Lee, J. Yang, S. Moon, S. Y. Lee, J. B. Shim, S. W. Kim, J. H. Lee, and K. An, "Observation of an exceptional point in a chaotic optical microcavity," Phys. Rev. Lett. **103**, 134101 (2009).
25. W. Gao, X. Li, M. Bamba, and J. Kono, "Continuous transition between weak and ultrastrong coupling through exceptional points in carbon nanotube microcavity exciton–polaritons," Nat. Photonics **12**, 362–367 (2018).
26. R. Uzdin, A. Mailybaev, and N. Moiseyev, "On the observability and asymmetry of adiabatic state flips generated by exceptional points," J. Phys. A **44**, 435302 (2011).
27. I. Gilary, A. A. Mailybaev, and N. Moiseyev, "Time-asymmetric quantum-state-exchange mechanism," Phys. Rev. A **88**, 010102 (2013).
28. T. J. Milburn, J. Doppler, C. A. Holmes, S. Portolan, S. Rotter, and P. Rabl, "General description of quasiadiabatic dynamical phenomena near exceptional points," Phys. Rev. A **92**, 052124 (2015).
29. A. U. Hassan, B. Zhen, M. Soljačić, M. Khajavikhan, and D. N. Christodoulides, "Dynamically encircling exceptional points: exact evolution and polarization state conversion," Phys. Rev. Lett. **118**, 093002 (2017).
30. J. Doppler, A. A. Mailybaev, J. Bohm, U. Kuhl, A. Girschik, F. Libisch, T. J. Milburn, P. Rabl, N. Moiseyev, and S. Rotter, "Dynamically encircling an exceptional point for asymmetric mode switching," Nature **537**, 76–79 (2016).
31. G. Lopez-Galmiche, H. E. Lopez Aviles, A. U. Hassan, A. Schumer, T. Kottos, P. L. LiKamWa, M. Khajavikhan, and D. N. Christodoulides, "Omnipolarizer action via encirclement of exceptional points," in *Conference on Lasers and Electro-Optics*, OSA Technical Digest (Optical Society of America, 2020), paper FM1A.3.

32. J. Fatome, S. Pitois, P. Morin, E. Assémat, D. Sugny, A. Picozzi, H. R. Jauslin, G. Millot, V. V. Kozlov, and S. Wabnitz, "A universal optical all-fiber omnipolarizer," Sci. Rep. **2**, 938 (2012).
33. L. Xiao, X. Zhan, Z. H. Bian, K. K. Wang, X. Zhang, X. P. Wang, J. Li, K. Mochizuki, D. Kim, N. Kawakami, W. Yi, H. Obuse, B. C. Sanders, and P. Xue, "Observation of topological edge states in parity–time-symmetric quantum walks," Nat. Phys. **13**, 1117–1123 (2017).
34. S. Weidemann, M. Kremer, T. Helbig, T. Hofmann, A. Stegmaier, M. Greiter, R. Thomale, and A. Szameit, "Topological funneling of light," Science **368**, 311–314 (2020).
35. L. Xiao, K. Wang, X. Zhan, Z. Bian, K. Kawabata, M. Ueda, W. Yi, and P. Xue, "Observation of critical phenomena in parity-time-symmetric quantum dynamics," Phys. Rev. Lett. **123**, 230401 (2019).